Synthesis and thermoelectric properties of rare earth Yb-doped Ba$_{8-x}$Yb$_x$Si$_{30}$Ga$_{16}$ clathrates

Lihua Liu [a,*], Feng Li [a], Yuping Wei [b], Ning Chen [b], Shanli Bi [b], Hongmei Qiu [a], Guohui Cao [b], Yang Li [a,c]

[a] University of Science and Technology Beijing, School of Mathematics and Physics, Department of Physics, Beijing 100083, China
[b] University of Science and Technology Beijing, School of Materials Science and Engineering, Beijing 100083, China
[c] University of Puerto Rico at Mayaguez, Department of Engineering Science and Materials, Mayaguez, PR 00681-9044, USA

ARTICLE INFO

ABSTRACT

The potential thermoelectric and magnetic application of clathrate materials with rare-earth doping is the focus of much of the recent research activity in the synthetic material physics and chemistry. A series of clathrate samples with the chemical formula Ba$_{8-x}$Yb$_x$Si$_{30}$Ga$_{16}$ ($x = 0, 0.5, 0.7, 1$ and 1.5) were prepared by combining arc melting, ball milling and spark plasma sintering (SPS) techniques. X-ray diffraction and scanning electronic microscopy combined with energy-dispersive X-ray spectroscopy (EDS) analysis showed the dominant phase to be the type-I clathrate. Whereas, X-ray structural refinement and EDS analysis indicated that some Yb atoms enter the clathrate lattice to replace Ba at $2a$ sites, while other Yb atoms are oxidized as Yb$_2$O$_3$ precipitated around grain boundaries. The solid solubility of Yb into clathrate lattice yielded $x \sim 0.3$. Comparative analysis between Yb-doped and Yb-free clathrates showed that the thermal conductivity decreases with Yb-doping. Consequently, thermoelectric figure of merit ZT significantly increased.

1. Introduction

In recent years, energy consumption and environmental pollution have emerged as some of the most critical issues. In traditional fossil fuel machinery, as much as 70% of the energy is squandered heat related entropy [1]. Therefore, enhancing energy efficiency has taken a center stage in the debate over environmental protection. In that regard, the study of thermoelectric materials has become a widely researched field as they can convert waste heat to electricity directly. The thermoelectric properties are generally expressed by the dimensionless figure of merit ZT as:

$$ZT = \frac{S^2\sigma}{\kappa}T \tag{1}$$

where S, σ, κ and T are Seebeck coefficient, electrical conductivity, thermal conductivity and absolute temperature, respectively. The higher energy conversion efficiency demands a larger ZT which requires a combination of high σ, S and T, and low κ simultaneously. However, optimizing the highly coupled parameters of Eq. (1) concurrently poses an arduous challenge.

A concept "phonon glass, electron crystal" (PGEC) has been introduced in 1995 referring to an ideal thermoelectric material that possess thermal properties similar to an amorphous solid while its electrical properties are similar to a single crystal semiconductor [2]. A widely studied class of PGEC compounds is clathrates [3,4]. Group-IV clathrate materials are extended Si, Ge and Sn cage-like solids with sp^3-hybridized networks [5–7]. These compounds have a semiconducting framework whereby the guest atoms like alkali-metal, alkaline-earth and rare-earth can be encapsulated into the cage. The covalently bonded framework promotes high electron mobility leading to reasonable values of electrical conductivity, whereas, the heat-carrying phonons are scattered effectively by the rattling of these guest atoms – it is the combination of these two factors that give rise to high ZT values for the clathrates.

As shown in Fig. 1, a typical type-I clathrates can be represented by the general formula A$_8$(IV)$_{46-x}$(III)$_x$ (space group $Pm\bar{3}n$), where A = K, Na, Rb, Cs, Sr, Ba, Eu, and III = Al, Ga, In, and IV = Si, Ge and Sn [8]. The substitution of the guest atom can greatly influence the thermoelectric properties. Recently, Prokofiev reported the successful incorporation of Ce as a guest atom into the clathrate crystal structure and observed a 50% enhancement of the thermo-power compared with a rare-earth-free reference material [9]. For type-I clathrates, the preferred stoichiometry is found to be A$_8$(IV)$_{30}$(III)$_{16}$ such as Ba$_8$Ge$_{30}$Ga$_{16}$, Ba$_8$Si$_{30}$Ga$_{16}$, Sr$_8$Ge$_{30}$Ga$_{16}$, Ba$_8$Si$_{30}$Al$_{16}$ and Eu$_8$Ge$_{30}$Ga$_{16}$. The bonding situation of A$_8$(IV)$_{30}$(III)$_{16}$ may be understood in terms of the so-called Zintl concept [10–13]. The guest atom in cages is assumed to be ionic and donate its valence electrons to the framework structure. In the Ba$_8$Si$_{30}$Ga$_{16}$ system for example, the 16 electrons donated by the eight Ba atoms can be accepted by the 16 group III Ga atoms. The ideal stoi-
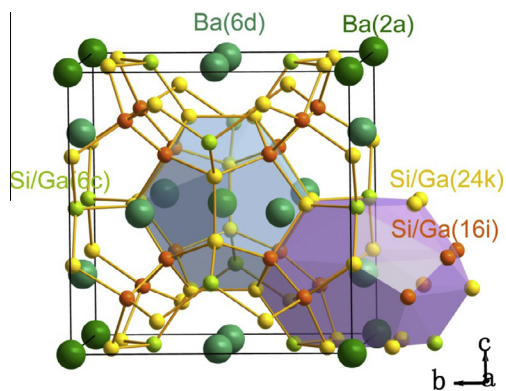
Fig. 1. The crystal structure of type-I clathrate $Ba_8Si_{30}Ga_{16}$ (space group $Pm\bar{3}n$) contains 20- and 24-atom polyhedra arranged on a simple cubic lattice.

chiometry $A_8(IV)_{30}(III)_{16}$ is expected to be semiconductor and therefore shows large thermopower. Among $A_8(IV)_{30}(III)_{16}$ clathrate systems, $Ba_8Si_{30}Ga_{16}$ clathrate has been well characterized and demonstrated to be a potential material for high temperature. Silicon is quite abundant and is cheaper than germanium and tin. Also, the higher melting point (about 1197 °C) and lighter weight of silicon are preferable for large scale industrial applications.

One of the primary approaches taken to improve the ZT value of clathrate is to lower lattice thermal conductivity. On the one hand, clathrate materials that contain heavy metal atoms in the cages are normally associated with low lattice thermal conductivity [14]. For example, the thermal conductivity is greatly suppressed when the guest atom is changed from Ba to Eu in Ge-base clathrates [15,16]. On the other hand, in the cages, two different kinds of metal atom fillings can interact with a wider spectrum of phonons than single atom filling, which has a significant effect on lowering the thermal conductivity [17,18]. By introducing rare earth Yb as guest atoms into clathrates $Ba_8Si_{30}Ga_{16}$, the thermoelectric properties would be improved as the Yb atom has a heavier mass and a smaller size.

To the best knowledge of the authors, no studies have yet been reported on the Yb doping in the Si clathrates. There are several reports on Yb-doping in Ge clathrates. Paschen reported the synthesis of polycrystalline $(Eu,Yb)_8Ge_{30}Ga_{16}$ clathrates by combining arc melting, annealing, high-speed melt spinning and spark plasma sintering process [19]. The XRD pattern of the sample show perfect single phase of clathrate and no trace of impurity phase. However, the higher resolution TEM technique revealed that there was no sizable substitution of Eu by Yb in the clathrate. In fact, Paschen observed that the Yb replaces Eu only in the foreign phase $EuGa_2$-Ge_2 or other amorphous and nanocrystalline inclusions of Yb-containing non-clathrate phases which would neither be detected by XRD nor by SEM. In addition, Tang et al. reported Yb/Sr and Yb/Ba double-atom-filled $Sr_{8-x}Yb_xGe_{30}Ga_{16}$ and $Ba_{8-x}Yb_xGe_{30}Ga_{16}$ clathrate synthesized by combining melting reaction with the spark plasma sintering method [20,21]. They provided Yb-doping amount in $Sr_{8-x}Yb_xGe_{30}Ga_{16}$ and $Ba_{8-x}Yb_xGe_{30}Ga_{16}$ of 0.7 and 1.0.

In this paper, the results of Yb-doping in $Ba_{8-x}Yb_xSi_{30}Ga_{16}$ clathrate are reported. The polycrystalline $Ba_{8-x}Yb_xSi_{30}Ga_{16}$ ($x = 0, 0.5, 0.7, 1$ and 1.5) clathrate samples were prepared by combining arc melting, mechanical milling and SPS methods. The crystallographic properties and composition distribution of the Yb on the dominant phase and grain boundary suggest that the Yb_2O_3 exists as an impurity phase on the grain boundary, which implies that a fraction of Yb ions entered clathrate lattice in Yb-doped specimens. The EDS analysis confirmed that in clathrates the average composition of Yb in one unit cell was 0.25–0.38. Whereas, the thermoelectric analysis provided a clear evidence of higher ZT values for

Yb-doped as compared with the Yb-free samples. The improvement of ZT is attributed to the decrease in the lattice thermal conductivity.

2. Experimental

A series of ingots with the chemical formula $Ba_{8-x}Yb_xSi_{30}Ga_{16}$ ($x = 0, 0.5, 0.7, 1$ and 1.5) were prepared by arc melting in argon from pure elements. Metals of Ba (99.99%), Ga (99.99%), Yb (99.999%) and Si (99.999%) were weighed. An extra amount (5%) of Ba was loaded considering Ba is more volatile and oxidable than other elements. The arc furnace chamber was evacuated to vacuum for more than 30 min and filled with pure argon. The metals Ba, Ga, Yb and Si were melted and reversed. This process was repeated four times to obtain good homogeneity. Then the ingots were ground into fine powder of size 0.1–3 μm by ball milling machine at a speed of 600 rpm for 30 min milling time. The dehydrated ethanol solvent was mixed with clathrate sample during ball milling to prevent fine powders from agglomeration. Finally, by using the spark plasma sintering (SPS) technique to obtain dense samples, the powders were sintered at 40 MPa for 10 min at 900 °C under an argon pressure of 10 Pa.

Powder X-ray diffraction (XRD) measurements were performed at room temperature in the 2θ range of 10–80° using Cu Kα radiation with a Rigaku DMAX-RB 12 KW diffractometer. Structural refinement of the powder X-ray diffraction data was carried out using the GSAS software package [22]. The chemical compositions were determined by scanning electron microscopy (XL30 S-FEG) combined with energy-dispersive X-ray spectroscopy (EDS). Electrical conductivity (σ) and Seebeck coefficient (S) were measured simultaneously using ULVAC ZEM-3 apparatus in a temperature range of 50–500 °C. The thermal diffusivity (α) and the specific heat (C_p) were measured by the flash method in Netzsch LFA 457 system under the temperature ranging from 50 to 500 °C. The densities (ρ) were measured by Archimedes drainage method. The relative density of the bulk obtained was more than 88%. Finally, measurements of Hall coefficients were performed at room temperature by using Quantum Design physical property measurement system (PPMS-9T).

3. Results and discussions

3.1. Crystalline structure and composition of Yb-doped clathrates

The X-ray diffraction patterns of nominal $Ba_{8-x}Yb_xSi_{30}Ga_{16}$ ($x = 0, 0.5, 0.7, 1$ and 1.5) compounds are shown in Fig. 2. In all diffraction patterns, no obviously observable peak from impurity phases was found. The lattice parameters of the samples were calculated by the least-squares method using the PowderX program [23]. The dominant phase was the type-I clathrate [cubic space group $Pm\bar{3}n$ (No. 223)] that could be indexed using $Ba_8Si_{30}Ga_{16}$ structure. The lattice parameter a of $Ba_{8-x}Yb_xSi_{30}Ga_{16}$ ($x = 0.7$) was obtained as 10.543(19) Å which is smaller than that of $Ba_{8-x}Yb_xSi_{30}Ga_{16}$ ($x = 0$) (10.551(23) Å). We know that the ionic radius of Yb^{2+} (0.858 Å) is less than the value of 1.35 Å for Ba^{2+}. However, we cannot definitely conclude that Yb is incorporated into the clathrate phase because the decrease of Ga content will also decrease the lattice parameters.
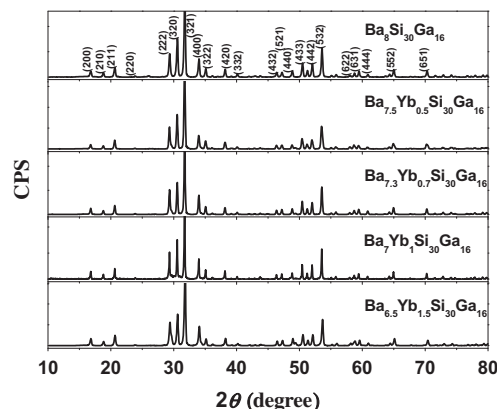

Fig. 2. X-ray diffraction patterns of the samples with nominal formula $Ba_{8-x}Yb_x$-$Si_{30}Ga_{16}$ ($x = 0, 0.5, 0.7, 1$ and 1.5).